

Volume and surface-area measurements using tomography, with an example from the Brenham pallasite meteorite

Jacob Spinsby^{a,*}, Heiner Friedrich^c, Peter R. Buseck^{a,b}

^a*School of Earth and Space Exploration, Arizona State University, Tempe, AZ, USA*

^b*Department of Chemistry and Biochemistry, Arizona State University, Tempe, AZ, USA*

^c*Inorganic Chemistry and Catalysis, Utrecht University, The Netherlands*

Received 28 September 2005; received in revised form 8 January 2007; accepted 18 January 2007

Abstract

Increased computer speed has helped to proliferate tomography throughout the geosciences. Although best known from the medical CATscan, tomography is also a powerful tool for geological problems. Whereas qualitative tomography is widely used, quantitative data from tomograms are not so commonly available. Presented here are two programs, Electron Tomography Segmentation, surface Area, and Volume (ETSAV) and Electron Tomography CUTter (ETCut), that were written to obtain quantitative volume and surface-area data from tomograms. Based on a specified threshold value, ETSAV distinguishes objects within a tomogram and then returns volume and surface-area data for each object. If object separation is unsatisfactory using a single threshold, ETCut is called to digitally separate objects that appear connected in the tomogram, allowing ETSAV to perform its functions. By knowing the nature of the object of interest, error can be corrected to, on average, less than 5% for a single object; combined volumes of many particles of different sizes may result in lesser errors. A section of the Brenham pallasite meteorite was examined using the programs. Olivine comprises 67.2% of the volume (50.4% wt%), followed by FeNi metal at 23.1% (39.3% wt%), troilite at 4.4% (4.8% wt%), and schreibersite at 3.4% (5.5% wt%). In all, 56.1% and 44.7% of the troilite and schreibersite surface areas, respectively, border olivine, suggesting that they wet olivine. Since the programs can be applied to any tomogram, from any field, there are many potential applications.

© 2007 Elsevier Ltd. All rights reserved.

Keywords: Tomography; Brenham pallasite; Quantitative tomography; Segmentation; Tomogram volume; Tomogram surface area; Fractal particles

1. Introduction

Advances in computing technology and speed, combined with decreased costs of powerful computers, have allowed tomography to become widely accessible. The principle of tomography, or the

creation of 3D data sets from multiple sets of 2D data, is familiar through the X-ray, computer-assisted tomography (CAT) scan used in the medical field (Hounsfield, 1972). It has been used to describe fractal particles (van Poppel et al., 2005), earthquakes (Chimera et al., 2003), Earth's deep interior (Lay et al., 1998), and meteorites (Lemelle et al., 2004) using techniques that include seismology (Lines, 1991), electron tomography (ET) (Bonetta, 2005),

*Corresponding author.

E-mail address: jspinsby@mchsi.com (J. Spinsby).

and X-ray computed tomography (XRCT) (Rowe et al., 1997).

Qualitative analysis of tomograms is relatively widespread, but quantitative analysis is less common. Existing programs written to digitally separate objects (a process called segmentation) ((Prousevitch and Sahagian, 2001) or methods used to calculate quantitative data from tomograms (Coker and Torquato, 1995) do not sufficiently address our problems. The reason is that they do not allow for individual surface area and volume measurements of individual objects, which are a function of both the segmentation and quantification approach. Recently, Ketcham (2005) described BLOB3D, a program designed to segment objects and then extract quantitative measurements. In our approach, segmentation and quantification are applied in one step, which offers a more direct and recursively applicable functionality: ETSAV, for Electron Tomography Segmentation, surface Area, and Volume, was created to uniquely identify objects in tomographic images and to calculate their volumes and surface areas. ETCut, for Electron Tomography CUTter, was created to digitally separate objects that appear connected to one another in the tomogram. Both programs have applications beyond ET and can scale to any tomogram representing any size; the names simply reflect their original purpose.

Both programs were written using Visual C++ 6.0 on a Windows 2000 system. They were compiled into .dll format so that they could be called using IDL (interactive data language; Research Systems, Inc.), a high-level programming language that can also act as a runtime environment for such files (Xie et al., 2003). The user inputs the required parameters in the initial call in IDL.

1.1. Tomogram data format and type

Transmission electron microscope (TEM), XRCT, and photographic images are 2D projections. These images contain pixels (picture elements), in which values are housed at unique positions specified by x and y coordinates. In contrast, a tomogram contains voxels (volume elements) (Argiro and Van Zandt, 1992), which use x , y , and z coordinates to describe the locations of specific values.

The most common type of data housed in a tomogram is grayscale, but the significance of the grayscale values depends on the method used to

acquire the tomogram. Tomograms acquired by stacking camera photographs have grayscale values that represent attenuated light, ET tomograms have grayscale values that represent attenuated electron intensity, and XRCT grayscale values represent X-ray attenuation.

2. ETSAV determinations

A typical tomogram consists of millions of voxels. A technique called thresholding is used to identify those voxels that comprise a specific phase or object within the tomogram. Based on a specified threshold value input by the user, a visualization program (e.g., Amira, www.amiravis.com) displays all voxels above that value and ignores all voxels below that value.

A threshold is chosen such that it identifies all voxels that comprise the phase(s) or object(s) of interest. An object can consist of many adjacent voxels, or may consist of just one. Voxels composing an object have many different values above the threshold, and the same voxel values are commonly present in multiple objects, leading to difficulty in identifying the individual objects. Although thresholding might allow two objects to appear separate in the visualization, the separated objects are not uniquely identified in the tomogram (Fig. 1A). However, each object must be distinguished in order to calculate its volume and surface area. A convenient method of distinguishing between different objects is to have each voxel of that object set to a specific value, and to use different values for different objects. This methodology is applied in ETSAV in the following way. In the first step, all voxels that have a value greater than or equal to the chosen threshold are reassigned to a value of 1. Voxels below the threshold are reassigned to 0.

In the second step, ETSAV searches systematically through the tomogram for a voxel with a value of 1, which is then referred to as the original voxel. The adjacent voxels are next searched to determine their values. Adjacent voxels with values of 1 and the original voxel form a group to which a unique object number is assigned—a sequential integer number starting with 2. As the search progresses through the array, a scan of the voxels adjacent to the original one may yield a value other than 1 or 0. If any adjacent voxel has a value greater than 1, it means that voxel had already been assigned an object number as part of an object. Thus, the original voxel and any adjacent ones with

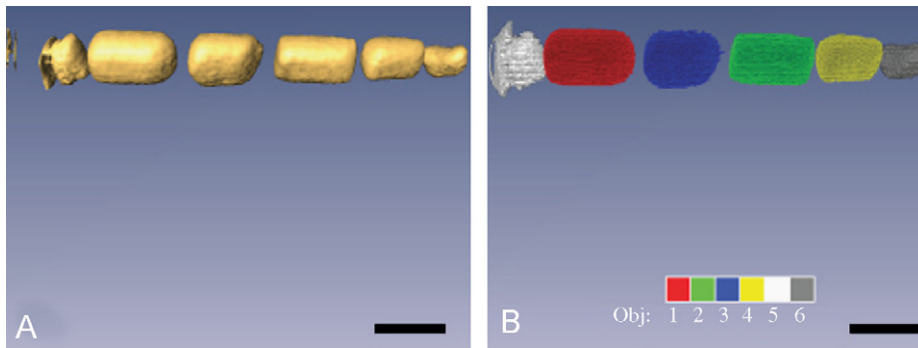


Fig. 1. Separation, or lack thereof, before and after using ETSAV. The left panel (A) shows magnetite crystals before being segmented. They are all of the same color because visualization software cannot distinguish among them. The right panel (B) shows the same magnetite crystals after ETSAV was applied. Each crystal has a different color, indicating that crystals are discrete objects. Scale bars represent approximately 50 nm.

a value of 1 are changed to match this new, incremented object number. This step assures that voxels adjacent to an existing object are assimilated into that object. Values are never changed for adjacent voxels with values of 0.

In rare cases, such as a U-shaped object, a search of the adjacent voxels may yield two separate object numbers (e.g., a voxel in one corner or end adjacent to the original voxel has a value of 2, and another adjacent voxel in an opposite corner or end has a value of 3). In this case, there is a logical conflict because if the value of the original voxel is changed to match one of the object numbers, then two separate object numbers will occur in two separate but adjacent voxels. If not corrected, this situation will yield at least two different voxel values for the same continuous object. To address this error, an entry is made into an internal 2-column array called the merge list. Each merge-list entry consists of the lowest object number as the first column entry and the remaining object number as the second column entry. In cases where more than two object numbers are found in a search of the voxels adjacent to the original voxel, multiple entries are made into the merge list. The merge list is stored for later use. The second step of ETSAV is repeated until there are no remaining voxels with a value of 1 left.

In the third step, ETSAV sorts the first column of the merge list in ascending order. The program starts with the entry at the bottom of the merge list and changes all voxels with the value in the right column to match the value in the left column. ETSAV moves up the list, until all entries have been examined. The array now contains assemblages that

consist of continuous voxels that all have the same value, defining an object. Volume and surface area can now be calculated.

The fourth step of ETSAV calculates the surface area and volume of all continuous objects in the tomogram. For each object, the program tallies the number of voxels that have that object number, which is returned as the volume (Fig. 2A). Surface area is calculated using two methods. Method 1 tallies the number of faces of voxels with a given value adjacent to the empty space (Fig. 2B). Method 2 tallies the number of voxels with a value of 0 immediately adjacent to voxels of an object (Fig. 2C). Accuracy was tested using a series of generated circles and squares. Each circle and square has known dimensions, and their volume and surface area can be calculated by hand and compared with the values calculated by ETSAV. Our tests show that method 2 is generally more accurate than method 1, but method 1 is still used for calculation as there are some objects in which it provides better results. A decision based on the shape of the object must be made to determine which surface-area measurement is likely to be more accurate. Error for both volume and surface area depends on the object being modeled, as objects with many curved surfaces yield higher errors, as do objects that have surfaces oriented at some angle other than 0 or 90 degrees to the grid. Generally, the accuracy of the volume and surface-area calculations increases with the number of voxels modeling a given object.

Since some object numbers that were originally used are now unused because of the merges carried out through the merge list, and since the assigned

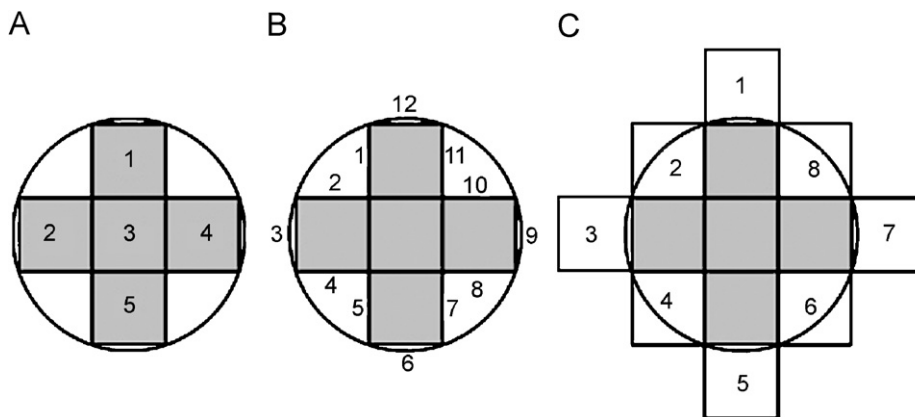


Fig. 2. Volume and surface-area calculations using 2D shapes. (A) represents how volume is calculated. (B) represents how surface-area method 1 is calculated. (C) represents how surface-area method 2 is calculated. One can also see the source of most of the error, as using squares to model a circle unavoidably produces error.

object numbers are based on the order in which they are found, the objects are not labeled in an easily identifiable scheme. In a fifth step, and to make the assignment of object numbers clearer, ETSAV sorts the objects by volume (from highest to lowest) and reassigns the object numbers accordingly (Fig. 1B).

A new tomogram is then saved that contains the voxel data from ETSAV. This new tomogram allows objects to be controlled individually, so that they can be (a) correlated with the volume and surface-area calculations written to a separate Excel file, and (b) visualized as unique objects. The volume and surface-area measurements can be converted to SI or any other desired units using a factor based on the scale of the tomogram, since they are initially output as raw voxel or face counts.

ETSAV can only distinguish separate objects that have empty space (voxels with a value of 0) between them. The occurrence of empty space between objects depends on the specified threshold. Lower thresholds permit more noise to be visible, perhaps connecting objects that would be separated at higher thresholds. In some cases, however, objects may not separate regardless of what threshold is chosen. This situation occurs, for example, when an object of interest is immediately adjacent to an object that is not of interest, and yet they both have the same physical property value used to threshold (density, X-ray attenuation, etc). ETCut is a separate program created to address this issue, although it may also be used for other purposes, such as cutting arms of fractal particles (e.g., of soot; van Poppel et al., 2005) to test for self-similarity.

3. Electron tomography cutter

The decision to use ETCut is made when the reconstructed tomogram is visualized to determine a threshold for use in ETSAV. The use of ETCut creates enough separation between objects to allow ETSAV to distinguish them. If object separation is satisfactory to the user at a given threshold, then ETCut is skipped, and ETSAV is implemented directly. If object separation is unsatisfactory (meaning some objects that are desired to be distinguished do not visually separate), then ETCut is called in a separate step before ETSAV.

Using Amira, the user determines three points (the minimum number needed to define a plane) that define the plane of separation, as well as a triangle that is a subset of the plane. The triangle is the portion of the plane where separation occurs, preventing situations where creating separation over the entire plane would separate complex object(s) of interest (e.g., a curved or U-shaped object) in undesirable places. It is necessary for ETCut to specify a width for the plane, and thus the triangle, since a plane is a 2D construction and tomograms consist of 3D voxels. In cases where the plane is parallel to two axes, it can be one voxel thick, and ETSAV can still distinguish the objects the plane separates. In all other cases, the plane must be thicker to allow ETSAV to distinguish the objects the plane separates. ETCut determines the necessary plane width so that it creates enough separation for ETSAV to distinguish objects. ETCut can only separate objects with a plane and so will not work as desired on objects that

are irregular such that they cannot be separated by a plane or a series of planes.

Thresholding is the first step in ETCut, and it is performed using the same process as in ETSAV. Once thresholding is complete, ETCut searches the array until a voxel with a value of 1 is found. The coordinates of the voxel are tested using a series of algebraic plane equations to determine if it is on the plane defined by the three input points.

If a voxel is on the plane, its value is changed to 2. After the first search run, all voxels with a value of 2 are polled, and the coordinates are tested using a series of algebraic triangle equations to determine whether they occur within the triangle. If so, their value is changed to 3. Four values are now present: voxel value 0 is for empty space, 1 is for voxels that are above the threshold, 2 is for voxels above the threshold and within the plane, and 3 represents the voxels where separation occurs (voxels above the threshold, on the plane, and within the triangle). The algorithm then polls voxels with a value of 3. Once found, the algorithm searches the adjacent voxels. All those voxels with a value of 2 are changed to 3. Thus, any object that the triangle intersects will be separated entirely along the plane. This procedure provides the user some leeway when choosing the three initial points. A new tomogram is created with all voxel values of 3 changed to 0, performing the separation and allowing ETSAV to distinguish the desired objects, and calculate volume and surface area for each object.

The ETCut process allows users to digitally separate objects that would not be able to be separated by thresholding alone. ETCut also allows users to define variable cut triangle sizes and orientations within the tomogram. Thirdly, ETCut incorporates a process that separates two objects along the defined plane even if all of the voxels necessary to separate the two objects are not contained within the triangle. This combination of functions makes ETCut valuable for many applications where thresholding and other separation techniques are not enough. Being able to call ETCut from IDL also allows more customization and recursive functionality. Additional details about ETSAV and ETCut can be found in Spinsby (2005).

4. Application to a sample of the Brenham pallasite meteorite

Pallasites are meteorites composed primarily of olivine and FeNi metal, with minor phases such as

troilite (FeS) and schreibersite ((Fe, Ni)₃P) (Buseck, 1977). Pallasites are especially interesting because olivine is intimately mixed with FeNi metal, a material with a far greater density, with no evidence of gravitational separation. Although there is uncertainty, the most popular theory is that pallasites represent the core–mantle boundary of their parent body (Kelly and Larimer, 1977; Urey, 1966).

A tomogram was created from a cuboid-shaped piece of the Brenham pallasite (Fig. 3) by assembling 41 archived images. The images are of serial sections that were prepared in 1969. The procedure was to polish the surface, etch it to highlight the structure in the metal, and then photograph it. Approximately 0.5 mm was then removed by grinding, and the process was repeated until the entire sample was consumed. In this case, physical sectioning was applied to create the tomogram. Other approaches work with projections (ET, XRCT), and yet another approach (con-focal light microscopy) uses optical sections.

After the photographs were digitized by scanning, the phases within each image had to be outlined manually because the grayscale value ranges for each phase varied among the original images, the grinding and polishing of the sample plucked out fragments and thereby turned the image black where the fragment was plucked, and grayscale ranges overlapped between some phases. ETSAV and ETCut were then used to produce the results in Table 1.

Olivine is the primary phase in our sample, comprising 67.2% of the volume (50.4% wt%), followed by FeNi metal at 23.1% (39.3% wt%), troilite at 4.4% (4.8% wt%), and schreibersite at 3.4% (5.5% wt%). The remaining 1.9% was likely left out during the manual segmentation of the images. The left column of Table 1 shows the volumetric and mass compositions of the sample.

The surface-area proportions are also shown in Table 1. The percentage of the total surface area of the phase is shown in the left column that borders the phase named in the top row. The sums of the rows yield 100% of the surface area of the given phase.

ETSAV can also be used to indicate whether a given phase is one large mass, or many small isolated masses. Olivine essentially forms one large, interconnected object. Ninety-five volume percent of the FeNi metal is in one continuous object, whereas schreibersite and troilite consist of several

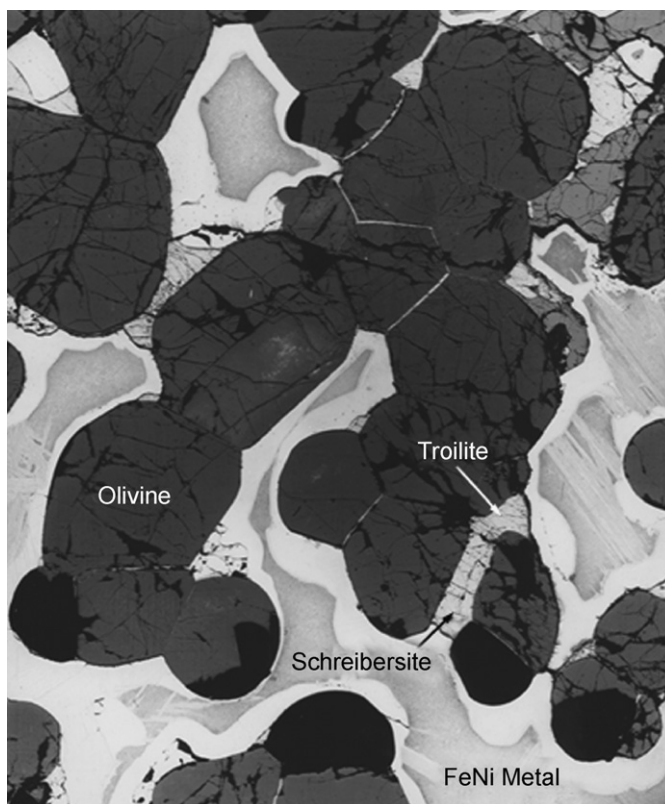


Fig. 3. A cross-sectional image representing one slice of a tomogram of the Brenham pallasite meteorite. Olivine grains are in a matrix composed of FeNi metal and are wetted by troilite and schreibersite.

Table 1
Quantitative data of our Brenham sample derived from ETSAV

	Olivine	Troilite	Schreibersite	FeNi metal
Olivine (67.2% vol%, 50.4% wt%)	×	26.5%	19.7%	53.9%
Troilite (4.4% vol%, 4.8% wt%)	56.1%	×	24.1%	19.8%
Schreibersite (3.4% vol%, 5.5% wt%)	44.7%	25.9%	×	29.4%
FeNi metal (23.1% vol%, 39.3% wt%)	70.7%	12.3%	17.0%	×

Phases are listed with their percent volume on the left. For surface areas, the table should be read as a percentage of the total surface area of the phase in the left column that borders the specified phase in the top row. Sums of rows yield 100%.

smaller objects. Forty percent of the total volume of schreibersite is within the largest object, 11.5% in its second largest object, and the remainder in smaller objects. Troilite is 32.5% contained in its largest object, 17.1% contained in its second largest object, followed by 9.6% and 4.3% for its other significant objects. The rest of the troilite is in smaller isolated pockets. If we treat troilite and schreibersite as a single phase for the purposes of understanding wetting of olivine when they were at higher temperatures and pressures, then the largest

object comprises 84.7%, indicating that schreibersite and troilite form an interconnected network. We believe it is reasonable to merge troilite and schreibersite into a single object in terms of their wetting properties against olivine, as in the individual serial sections both appear to similarly wet olivine.

Knowledge of the precise volumetric makeup, as well as the adhesion and wetting properties of the phases within Brenham, may contribute to understanding the history of this and related meteorites

and shed light on their potential relevance to the history of their parent body.

5. Conclusions

The ideas and methods presented in this paper are applicable to all fields of tomography, not just tomography in the geosciences. ETSAV and ETCut can scale to any tomogram representing any size of any object. They have already been applied to other projects such as atmospheric soot (van Poppel et al., 2005) and in the search for diamonds in diamond-bearing peridotite samples using XRCT. Quantitative data obtained using this technique are accurate, especially if a correction factor derived from simulated objects is used. These programs represent a step towards making quantitative tomography, and tomography in general, more useable for scientists in all fields.

Acknowledgements

This paper describes work carried out at the Arizona State University under Grant EAR-0440388 from the NSF Earth Sciences Division and NNG06GF08G from the NASA Cosmochemistry Program. We thank Steven A. Gordon and the Software Factory for their programming help, Gary Scott for his work in preparing the Brenham sections and photographs many years ago, and Laura van Poppel for her work in calibrating and testing ETSAV and ETCut.

References

- Argiro, V., Van Zandt, W., 1992. Voxels: data in 3-D. *Byte* 17, 177–182.
- Bonetta, L., 2005. Zooming in on electron tomography. *Nature Methods* 2, 139–145.
- Buseck, P.R., 1977. Pallasite meteorites—mineralogy, petrology, and geochemistry. *Geochimica et Cosmochimica Acta* 41, 711–740.
- Chimera, G., Aoudia, A., Sarao, A., Panza, G.F., 2003. Active tectonics in central Italy: constraints from surface wave tomography and source moment tensor inversion. *Physics of the Earth and Planetary Interiors* 138, 241–262.
- Coker, D.A., Torquato, S., 1995. Extraction of morphological quantities from a digitized medium. *Journal of Applied Physics* 77, 6087–6099.
- Hounsfield, G.N., 1972. A Method and Apparatus for Examination of a Body by Radiation such as X or Gamma Radiation. The Patent Office, London, England (British Patent Number 1283915).
- Kelly, W.R., Larimer, J.W., 1977. Chemical fractionation in meteorites—VIII. Iron meteorites and cosmochemical history of the metal phase. *Geochimica et Cosmochimica Acta* 41, 93–111.
- Ketcham, R.A., 2005. Computational methods for quantitative analysis of three-dimensional features in geological specimens. *Geosphere* 1, 32–41.
- Lay, T., Williams, Q., Garnero, E.J., 1998. The core–mantle boundary layer and deep earth dynamics. *Nature* 392, 461–469.
- Lemelle, L., Simionovici, A., Truche, R., Rau, C., Chukalina, M., Gillet, P., 2004. A new nondestructive X-ray method for the determination of the 3D mineralogy at the micrometer scale. *American Mineralogist* 89, 547–553.
- Lines, L.R., 1991. Applications of tomography to borehole and reflection seismology. *Society of Exploration Geologists Abstracts* 61, 102.
- Proussevitch, A.A., Sahagian, D.L., 2001. Recognition and separation of discrete objects within complex voxelized structures. *Computers & Geosciences* 27, 441–454.
- Rowe, T., Kappelman, J., Carlson, W.D., Ketcham, R.A., Denison, C., 1997. High-resolution computed tomography: a breakthrough technology for earth scientists. *Geotimes* 42, 23–27.
- Spinsby, J., 2005. *Mineralogical Applications of Tomography*. Master's Thesis, Arizona State University, Tempe, Arizona, USA, 76pp.
- Urey, H.C., 1966. Chemical evidence relative to the origin of the solar system. *The Geophysical Journal of the Royal Astronomical Society* 131, 199–223.
- van Poppel, L.H., Friedrich, H., Spinsby, J., Chung, S.H., Seinfeld, J.H., Buseck, P.R., 2005. 3D morphology of soot—implications for atmospheric lifetimes and radiative forcing. *Geophysical Research Letters* 32, 24461–24464.
- Xie, H., Hicks, N., Keller, G.R., Huang, H., Kreinovich, V., 2003. An IDL/ENVI implementation of the FFT-based algorithm for automatic image registration. *Computers & Geosciences* 29, 1045–1055.